WORLD JOURNAL OF PHARMACY AND PHARMACEUTICAL SCIENCES
SJIF Impact Factor 6.041
Volume 5, Issue 4, 196-213 Research Article ISSN 2278 – 4357

A 3D BIOPRINTING LIVER TUMOR MODEL FOR DRUG SCREENING

Xinwei Zhou[1#], Chang Liu[2#], Xinru Zhao[1], Xiaohong Wang [1,2]*

[1]Center of Organ Manufacturing, Department of Mechanical Engineering, Tsinghua University, Beijing 100084, P.R. China.

[2]Tianjin Power Technology Company Limited, Tianjin 301701, P.R. China.

Article Received on
26 Jan 2016,
Revised on 17 Feb 2016,
Accepted on 11 Mar 2016
DOI: 10.20959/wjpps20164-6311

***Correspondence for Author**
Dr. Xinwei Zhou
Center of Organ Manufacturing, Department of Mechanical Engineering, Tsinghua University, Beijing 100084, P.R. China.

ABSTRACT

Building a three-dimensional (3D) tissue model *in vitro* instead of animal models to test drug sensitivity has been an inevitable trend in drug research and development for it is less expensive, less time consuming, and more tightly controlled. In this article, a 3D liver tumor model consisting of HepG2 cells and sodium alginate/gelatin/fibrinogen hydrogel was created using a cell 3D bioprinter developed in Tsinghua University our own group. The subsequent scanning electron microscope observation and acridine orange/propidium iodide staining results indicated that HepG2 cells loaded in the alginate/gelatin/fibrinogen hydrogel grew well with high cell livability. Cell Count Kit-8, alpha-fetoprotein and half maximal inhibitory measurements demonstrated and verified that under the treatment of different anti-cancer drugs, such as 5-Fluorouracil, mitomycin and their combination, significant differences between the HepG2 cell behaviors in the 3D and 2D conditions were existed. The 3D liver tumor model is a promising application for *in vitro* drug screening.

KEYWORDS: 3D cell bioprinting; drug screening; liver tumor model; HepG2 cells; 2D cell culture.

INTRODUCTION

Drug screening is an indispensable process for drug effectiveness evaluation and development, especially for anti-cancer drugs. Over the past decades, *in vitro* cell culture models have got increasing attention in drug discovery progresses, for their less expensive,

less time consuming, more tightly controlled and high-throughput when compared with *in vivo* animal models.[1] *In vitro* cell culture models are indeed beneficial to systematic, repetitive and quantitative cell behavior research during drug screening.

Conventional cell culture in two-dimensional (2D) monolayer has been consistently utilized in drug screening for several decades. This technique has made significant contributions to biological and pharmaceutical research due to its easily manipulation and adaption properties.[2,3] However, cells of body *in vivo* are all in a complex three-dimensional (3D) environment in which different cells signal each other by transferring various proteins and genes, which cannot be realized in simple 2D architectures. There are existing significant differences between biological properties expressed by cells in 2D and 3D conditions.[4] Additionally, the lack of the counterpart *in vivo* 3D extracellular matrix (ECM) networks hinder the experimental drug screening effects, with even contradictory and misleading results.[2,5] Thus, most of the promising results acquired from 2D cell culture experiments usually cannot match those found *in vivo* settings.[6] To overcome these problems, 3D culture systems, an artificially-created environment in which biological cells are permitted to grow or interact with its surroundings in all three dimensions, have been established and developed.[7] Comparing with 2D cell cultures, 3D cell cultures can provide a cellular microenvironment that is more similar to the native *in vivo* environment. This feature is extremely vital in drug screening since environmental cues can affect cell properties, behaviors, and functions so as to affect cellular responses and sensitivity to drugs.[8,9] So creating 3D *in vitro* cell culture model, insteading of simple 2D cellular platforms, is an inevitable trend in drug screening.[10]

There are a number of techniques to creating 3D cell culture models *in vitro*, including roughly cell spheroids, microcarrier cultures, micropatterned surfaces, tissue engineering methods, etc.[11], among which tissue engineering approaches have been paid much more attention over the past years. Relying on seeding cells onto some pre-fabricated scaffolds, conventional tissue engineering methods have presented more and more disadvantages, such as cell peeling off, difficult to form tissues, and so on. Furthermore, it is extremely difficult to use the conventional tissue engineering methods to accurately define and arrange multiple cell types in one construct[12], which could be properly solved by 3D bioprinting techniques.

3D bioprinting, also called rapid prototyping (RP) or additive manufacturing (AM), comprises a series of techniques that can simultaneously assemble cells and ECMs from digital models in a precisely controlled layer-by-layer fashion.[13-20] Derived from industrial

application, 3D bioprinting has been transformed to assemble or print cells to form tissues as 3D drug screening models by many research groups. For example, Gaetani and coworkers have created a cardiac tissue with high cell livability via bioprinting human cardiac-derived cardiomyocyte progenitor cells and biomaterials.[21] In our own research group, we have developed a series of 3D bioprinting techniques which have been successfully used for *in vitro* tissue and organ manufacturing, giving a promising future for drug screening model establishment.[22-32]

In the present report, we made a 3D cell printing liver tumor model using one of our cell 3D printers for drug screening. HepG2 cells loaded in a hydrogel consisting of sodium alginate, gelatin and fibrinogen. The 3D liver tumor model was characterized for cell survival states after printing. Several anti-cancer drugs were used to test drug sensitivities to the HepG2 cells with the control of HepG2 cells cultured in 2D monolayers.

MATERIALS AND METHODS

Material preparation

Based on our former researches, sodium alginate, fibrinogen and gelatin were chosen to be the ECM in the present study.[33-39] Sodium alginate (Sinopharm Chemical Reagent Co., Ltd, SCRC, China) and gelatin (Tianjin Green-Island Company, China) were respectively dissolved in calcium-free phosphate buffered saline (PBS) to form 5% (w/v) and 20% (w/v) solutions. Fibrinogen (Sigma, Aldrich Company, USA) was dissolved in fetal bovine serum (FBS; Sijiqing, Beijing, China)-free Dulbecco's Modified Eagle's Medium (DMEM; Gibco, Vienna, VA, USA) to form a 5 % (w/v) solution. The sodium alginate, gelatin, fibrinogen solutions were mixed in a volume ratio of 2:2:1 before being pasteurized three times at 70℃ for 20 min. Bovine thrombin (Gibco, Santa Cruz, CA, USA) and calcium chloride ($CaCl_2$) was dissolved in PBS to give a final concentration of 100 IU/mL and 2% (w/v) individually.

HepG2 cells were purchased from Shanghai Institutes for Biological Sciences (SIBS) and cultured in minimum essential medium (MEM; Gibco, Vienna, VA, USA) supplemented with 10% FBS, 200 kU/L penicillin and 100 mg/L streptomycin and maintained at 37°C and 5% CO_2. The medium was changed every second day.

Construction of the liver tumor model using a 3D cell printer

Developed by our research group, the 3D cell printer is a kind of direct 3D controlled assembling technique. Temperature sensitive hydrogel, such as the sodium

alginate/gelatin/fibrinogen, loading with living cells was positioned precisely layer-by-layer and eventually formed a predefined 3D cell-matrix structure (Figure 1).[12] In this article, HepG2 cells, loaded into the sodium alginate/gelatin/fibrinogen hydrogel, at a density of 5×10^6 cells/mL, were printed, formed a 3D structure of 10 mm × 10 mm × 5 mm. After being printed, the construct was stabilized with a 5% (w/v) $CaCl_2$ solution and a 100 IU/mL thrombin solution separately for 5 min in order to crosslink the sodium alginate and to polymerize the fibrinogen molecules.

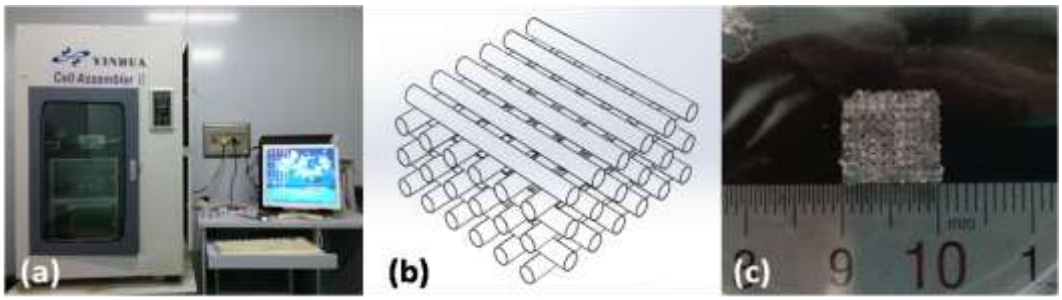

Figure 1. The cell printer (a), a computer-aided designed model (b), and a grid 3D cell-laden construct (c) [12].

Characterization of the printed liver tumor model

The state and behavior of the cells in the printed liver tumor model were characterized through scanning electron microscope (SEM) observation, acridine orange (AO)/propidium iodide (PI) staining, Cell Counting Kit-8 (CCK-8) method and alpha-fetoprotein (AFP) assay. SEM is a type of common electron microscope that produces images by scanning the object with a focused beam of electrons, supplying detailed information about the object's surface topography and composition. The printed liver tumor model samples after culturing for certain time were handled according to the previous described method [12], and observed using a SEM (Hitachi S-450, Japan). AO/PI staining is a general method to observe the living or dead state of the cell. The living cell would present green while dead cells dyed red in laser scanning confocal microscope (LSCM, LSM710-3channel, Zeiss, Germany) with AO-PI staining. CCK-8 method is an accurate and simple strategy to measure the amount of living cells, especially in cell proliferation and toxicity measurements.[40] The AO/PI staining and CCK-8 measurement steps were the same as that described in the previous article.[12] AFP is a kind of glycoprotein, which is nearly disappeared in healthy adult but widely enhanced in liver cancer patients. AFP has been an important serum biomarker to diagnose hepatocellular carcinoma (HCC) in clinic for nearly 50 years.[41,42] The AFP assay was done in clinical laboratory of hospital Tsinghua University.

Drug screening

Two common anti-cancer drugs, including mitomycin (MMC, Sigma, USA) and 5-Fluorouracil (5-FU, Sigma, USA), and their combination (MMC + 5-FU) were utilized herein to test the sensitivity of the liver tumor model. These anti-cancer drugs were dissolved in MEM containing 10% FBS with the following concentrations (Table 1).

Table:1. Working concentrations of the anti-cancer drugs

Drugs	MMC	5-FU	MMC+5-FU
Concentration (μg/mL)	3	50	3+50

The CCK-8 method and AO/PI staining were utilized to observe the state of HepG2 cells in the treatment of anti-cancer drugs quantitatively and qualitatively. As control groups, the HepG2 cells were cultured in 24-well plate (2D condition) with the concentration of 1×10^5 cells/mL and performed the same treatment.

The cell livability (CL) in this paper was calculated by the following formula:

$$\mathrm{CL} = \frac{OD_i}{OD_j} \times 100\%$$

Where OD_i was the optical density of the objects (i.e. 3D liver tumor model or 2D HepG2 cells) cultured in solutions with anti-cancer drugs. OD_j is the optical density of the corresponding objects cultured in solutions without anti-cancer drugs.

Additionally, half maximal inhibitory concentration (IC50) was measured to represent the drug sensitivity of the HepG2 cells in the 3D liver tumor model or 2D plate monolayer condition. IC50 was the drug concentration that exactly inhibited a given biological process by half. It is an index measuring the effectiveness of a substance in inhibiting a specific biological or biochemical function. The steps to measure the IC50 of the HepG2 cells either in the 3D liver tumor model or 2D plate monolayer were the same as that of the CCK-8 method. After the HepG2 cells in the 3D liver tumor model and 2D plate monolayer were treated in the solutions containing corresponding anti-cancer drugs with the concentrations of the Table 2. Cell livability was measured after 24 h culturing through CCK-8 method. The IC50 values, corresponding 50% of the cell viabilities, were then calculated according to the drug concentrations using a curve fitting method.

Table:2. Drug concentrations corresponding the IC50

Drug concentration (μg/mL)	1	2	3	4	5
MMC	0.3	3	30	50	80
5-FU	5	50	250	500	1000

RESULTS

Scanning electron microscopic observation of the 3D liver tumor model

Figure 2a-2f show a series of SEM images of the 3D liver tumor model after culturing for 1, 7 and 13 days. The surface morphology and spatial distribution of the HepG2 cells and sodium alginate/gelatin/fibrinogen matrix material were clearly observed. A lot of micropores were detected in the sodium alginate/gelatin/fibrinogen hydrogel after freeze-drying. The matrix material provided a suitable 3D circumstance which is benefit to the cell growth. The average size of the HepG2 cells was about 10μm in diameter. The surfaces of the HepG2 cells were roughness with plentiful microvilli (i.e. sodium alginate/gelatin/fibrinogen fibers) connecting the cells. Abundant cells in divisions and cell clusters were observed in the 7 and 13 days culture samples. Comparing with the 2D monolayer cell cultures after different time periods cell clusters formed via cell migration and proliferation in the SEM images of the 3D liver tumor model (Figure 2a, 2c, 2e), became larger and larger over the time, demonstrating that HepG2 cells established connections easily in the sodium alginate/gelatin/fibrinogen matrix material. Especially, there appeared many cell clusters more than 50μm in diameter in the 3D liver tumor model after 13 days culture.

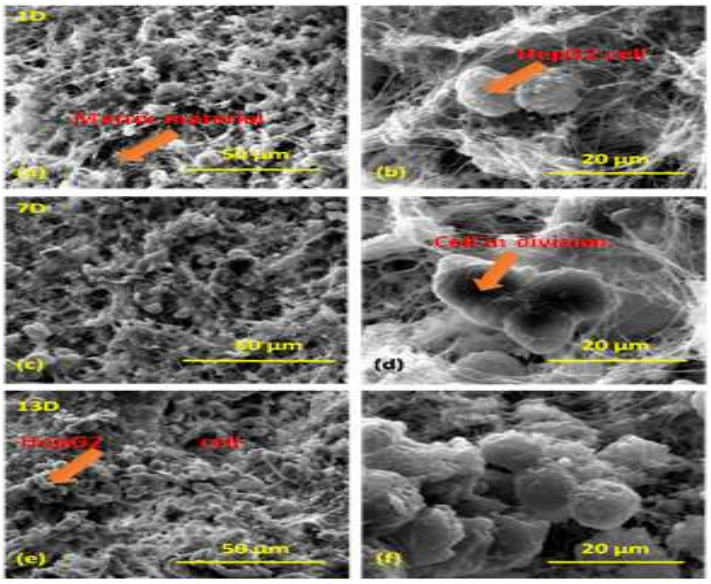

Figure 2 Scanning electron microscope images of the 3D liver tumor model. (a) Liver tumor model after 1 day culture; (b) The enlarged partial image of (a);(c) Liver tumor

model after 7 day culture; (d) The enlarged partial image of (c); (e) Liver tumor model after 13 day culture; (f) The enlarged partial image of (e);

AO/PI staining

AO/PI staining results of the HepG2 cells in the 3D liver tumor model are shown in Figure 3. In general, the printed HepG2 cells were all alive (green, 100% cell livability) with no dead cell (red) even after 14 days' culture. After 3 days culture, HepG2 cells in the 3D liver tumor model existed in the form of a single cell or cell group consisting of less than five cells, scattering without tight links spatially. Most of the cell nuclei were round and intact with bright green color for the hyaline globules (HG) (Figure 3a, 3b). After 7 days' proliferation and migration, the sizes of some cell clusters increased nearly to 50 μm in diameter (Figure 3c). With the culture time prolonging, the amount and size of the cell cluster were increasing (Figure 3e, 3f). However the color of the HG in the HepG2 cells was gradually diminished, indicating the decrease of the cell activities.

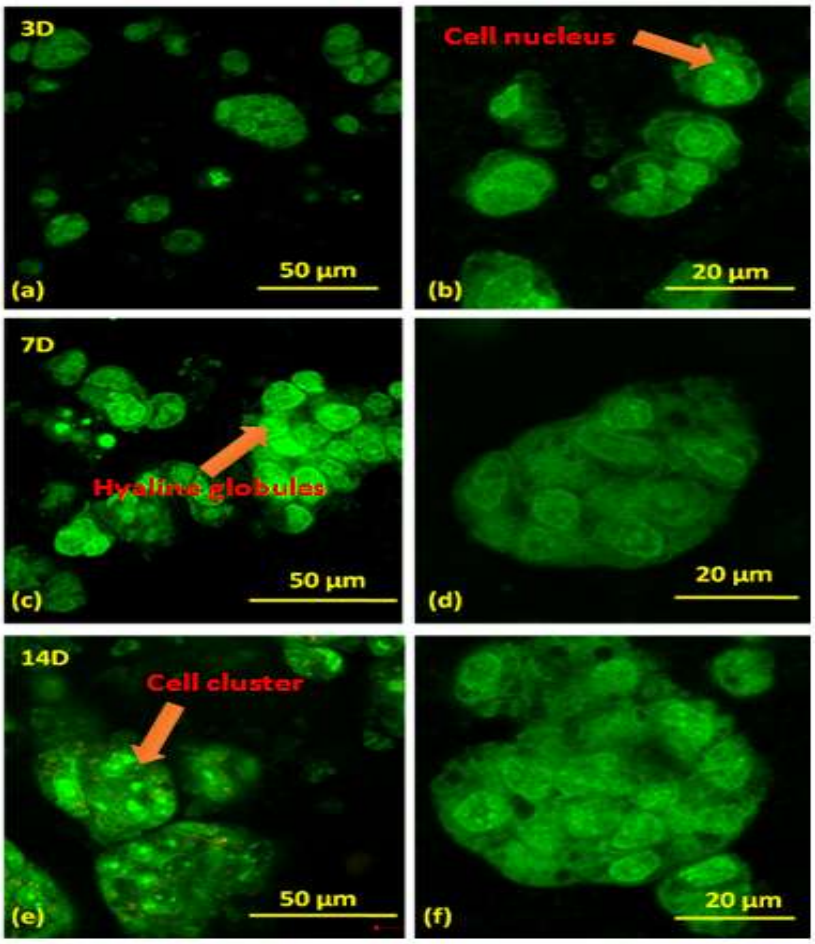

Figure 3 AO/PI staining images of the HepG2 cells in the 3D liver tumor model. (a) Liver tumor model after 3 days culture; (b) The enlarged partial image of (a); (c) Liver

tumor model after 7 days culture; (d) The enlarged partial image of (c); (e) Liver tumor model after 14 days culture; (f) The enlarged partial image of (e).

AFP assay and cell proliferation levels

The AFP assay and cell proliferation levels of the HepG2 cells in the 3D and 2D conditions are respectively shown in Figure 4. Both the AFP assay results of the HepG2 cells in the two conditions increased to certain levels before reduced over time (Figure 4a). It is interesting that both of the AFP levels in the two conditions almost disappeared at the eleventh day. The AFP level of the HepG2 cells in the 3D liver tumor model (3D condition) was significant lower than that in the 2D monolayer culture (2D condition, Figure 4a). As for the living cells, HepG2 cells in the 3D condition experienced a considerably growth in number, while in the 2D condition increased a little before decreased constantly in the first 10 days of culture (Figure 4b). Cell density in the 3D liver tumor model was much higher than that of the control 2D condition, while AFP level in the control 2D condition was only about 1/9 of the 3D liver tumor model after 5 days of culture. This result may be interpreted by that different cell culture models (2D and 3D) could lead different AFP expression. Compared with the 2D culture, HepG2 cells in the 3D printed liver tumor model was much closer to the native 3D environments, which could provide more realistic experimental results for the study of the AFP expression mechanism.

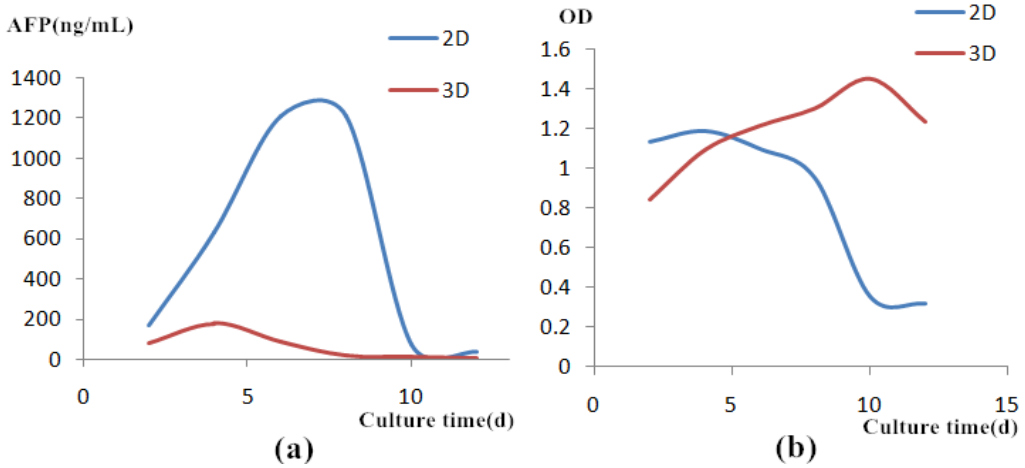

Figure 4 AFP assay (a) and cell proliferation level (b) of the HepG2 cells in 3D and 2D conditions.

Drug screening

Figure 5 reveals the drug screening results of the anti-cancer drugs in the working concentrations shown in Table 1. HepG2 cells in the 2D condition were more resistant to

MMC than that of the cells in the 3D culture, while the resistance of the HepG2 cells in the 3D condition to 5-FU was stronger (Figure 5). So we set another combination group that HepG2 cells in 2D and 3D conditions were cultured in MEM solution with the combined drugs of MMC and 5-FU. In the combination group, HepG2 cell livability in 2D condition was much higher than that in the 3D condition in the first one culture day, and tended to be consistent after 48 h culture (Figure 5). It was concluded that the MMC took the main effect at the first 24 h, while the 5-FU took the main effect during the following 24 h. There was a significant difference of cell responses to the same drugs, in different conditions (2D and 3D).

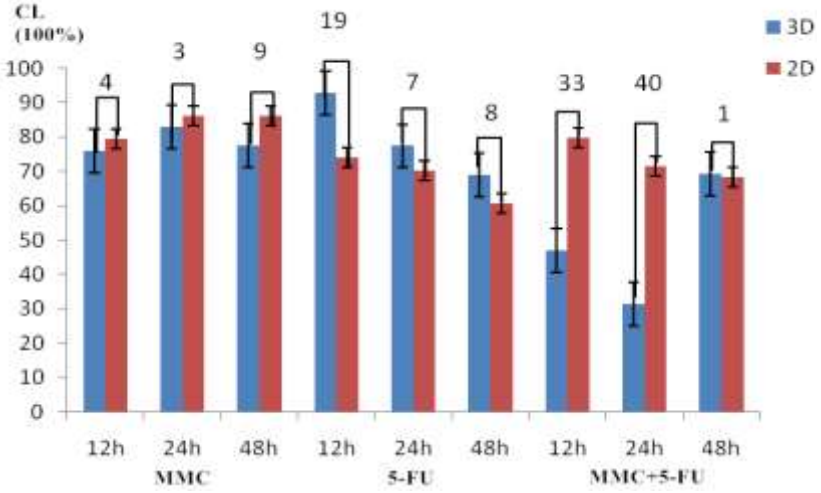

Figure 5 Drug screening results of the MMC, 5-FU, and MMC+5-FU.

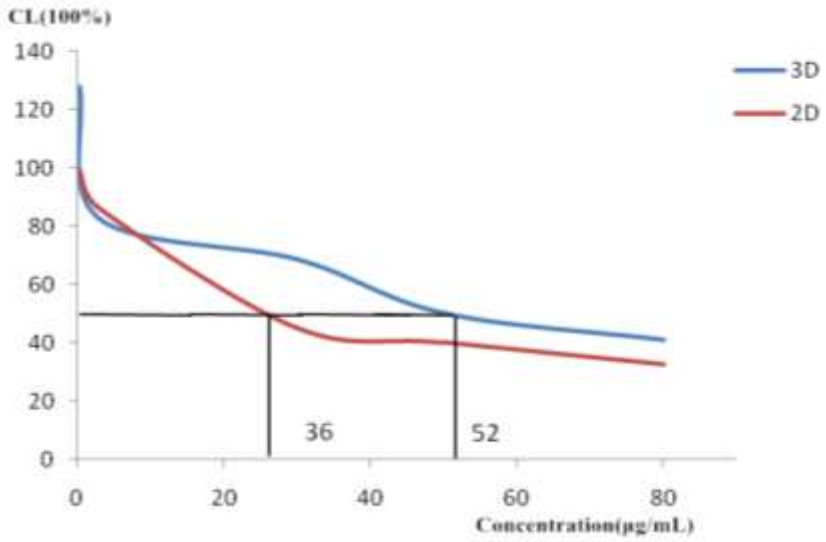

Figure 6 Fitting curves of the cell livabilities and MMC concentrations in different culture conditions.

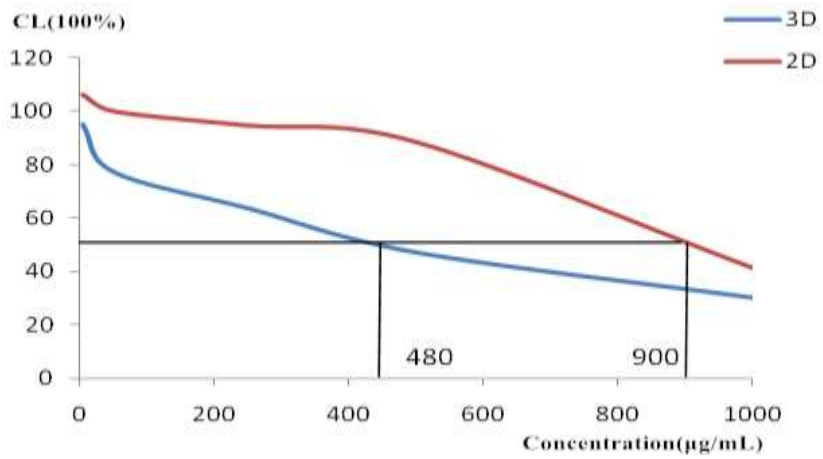

Figure 7 Fitting curves of the cell livabilities and 5-FU concentrations in different culture conditions.

IC50 results of the MMC and 5-FU are presented in Figure 6 (MMC) and Figure 7 (5-FU). Correspondingly, the IC50 values which were obtained from the relevant curves via curve-fitting and interpolation are shown in Table 3.

Table 3 IC50 of the anti-cancer drugs for the HepG2 cells in different culture conditions.

IC50(μg/mL)	MMC	5-FU
2D	36	900
3D	52	480

Similar to the results shown in Figure 5, HepG2 cell livability in the 3D condition was a little more than that in the 2D condition when treating with the same concentrations of MMC, demonstrating that the HepG2 cell in the 3D condition had a slight stronger resistance to the MMC. The IC50 of the MMC for the HepG2 cells cultured in the 3D condition (52 μg/mL) was a little more than that in the 2D condition (36 μg/mL) (Table 3). The two cell livability curves had the similar shapes and trends (Figure 6). Thus, the HepG2 cell responses to the MMC in 3D and 2D conditions were not obvious. However, the result was contrary for the drug 5-FU, shown in Figure 7. The curve in 3D condition was quite different from that in the 2D condition and the HepG2 cell livability of the 3D condition was much less than that of the 2D condition. Although the two curves had the same trend, the weak resistance of cells in the 3D condition to 5-FU is obvious. Furthermore, the IC50 of the 5-FU for the HepG2 cells cultured in the 3D condition (480 μg/mL) was only half of that in the 2D condition (900 μg/mL). Huge difference indicated that the 2D culture enhanced the drug resistance of

HepG2 cells to 5-FU, and this couldn't mirror truly the drug action mechanism of the cells in the 3D structure.

To further certify this ratiocination, we utilized AO/PI staining to view the HepG2 cell survival states directly in the presence of anti-cancer drugs. The staining images were presented in Figure 8 and Figure 9 with comprehensive results of drug screening in the 2D and 3D conditions. Figure 8 is the AO/PI staining result of the HepG2 cells in the 3D liver tumor model after one day *in vitro* culture under the influence of anti-cancer drugs or not. Figure 8a was the control group in the absence of any anti-cancer drug. From the staining images, HepG2 cells grew in very good condition with little dead cell and formed abundant cell clusters in the control group without any anti-cancer drug (Figure 8a). In the treatment of MMC (Figure 8b) or 5-FU (Figure 8c), HepG2 cells also formed many cell clusters, but there were considerable dead cells in the cell clusters. More dead cells were viewed in the group with the combined anti-cancer drugs of MMC and 5-FU, with the organizational structure of cell clusters remained complete. In the 3D liver tumor models, the death of the whole tumor models typically started from some cells, then developed to the cell cluster and finally to the whole 3D tumor models. So the drug effects for the HepG2 cells in 3D condition were not uniform. Cells in the surface of the cell cluster were more vulnerable to the drugs than those in the interior of the 3D liver tumor models.

Figure 9 presents the AO/PI staining results of the HepG2 cells in the 2D condition after one day *in vitro* culture with or without the effects of anti-cancer drugs. HepG2 cells grew in a relatively uniform way at the bottom of the culture dishes. There was nearly no dead cell in the control group without drug treatment (Figure 9a). Nevertheless, quite a few flaky dead cells appeared in the presence of MMC (Figure 9b) and 5-FU (Figure 9c). There were only a few independent cells left after the dead cells fall off from the bottom of the culture dishes with the combined treatment of the of MMC and 5-FU. The death cells were also raised locally and spread to all cells in the 2D condition. The non-homogeneity of the dead cell distribution was slighter than that in the 3D condition.

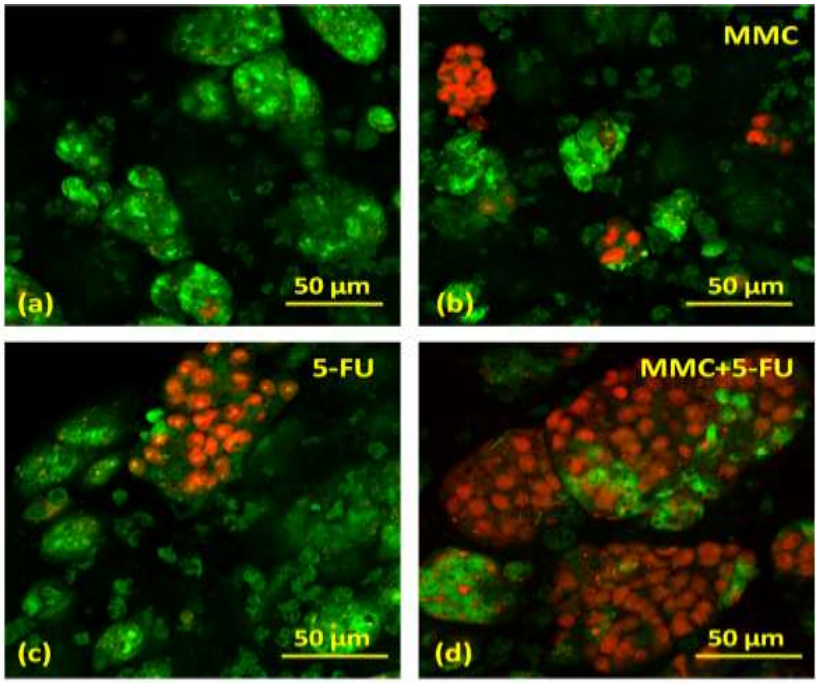

Figure 8 AO/PI staining results of the HepG2 cells after 1 day culture in the 3D liver tumor model with or without the interferences of anti-cancer drugs. (a) HepG2 cells without any drug. (b) HepG2 cells under the treatment of MMC. (c) HepG2 cells under the treatment of 5-FU. (d) HepG2 cells under the treatment of the combined MMC and 5-FU.

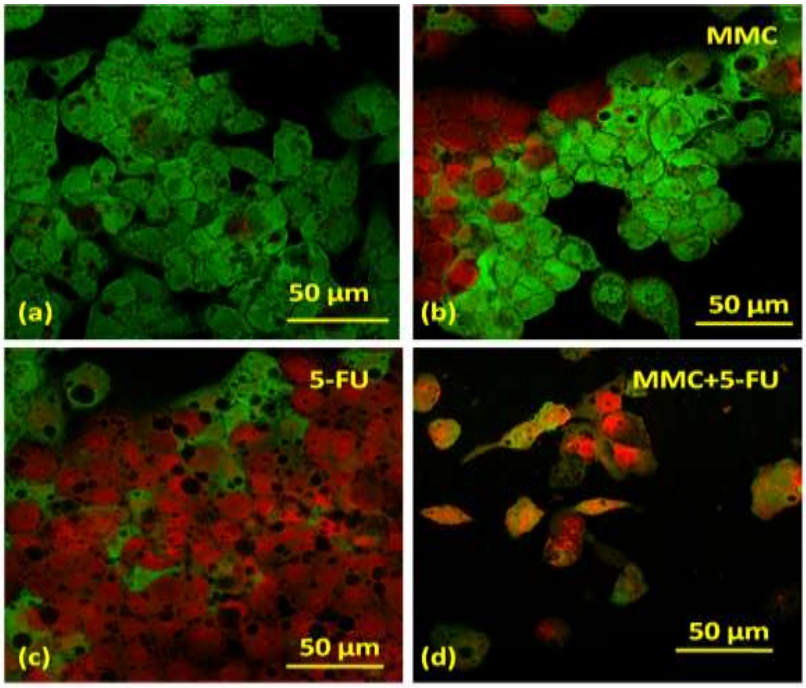

Figure 9 AO/PI staining results of the HepG2 cells after 1 day culture in 2D condition with or without the interferences of anti-cancer drugs. (a) HepG2 cells without any

drug. (b) HepG2 cells under the treatment of MMC. (c) HepG2 cells under the treatment of 5-FU. (d) HepG2 cells under the treatment of combined MMC and 5-FU.

DISCUSSION

Currently, most types of cancers in advanced stages are not curable by merely chemotherapy, and new drug discovery and development still continue to play an important role in the fighting against cancers. Liver cancer, a cancer that originates in the liver, remains to be the fifth most common malignancy in men and the eighth in women worldwide [43], damaging greatly the health of human. So testing the effectiveness of anti-cancer drugs is an urge but meaningful work. Conventional animal model has the disadvantage of costly and time-consuming, while the simple 2D cell model cannot mimic the cancer model *in vivo* effectively. Creating 3D tissue model *in vitro* for drug screening has been an important part in tissue engineering and organ manufacturing.

3D cell printing is an intelligent freeform fabrication technique that can automatically generate a sophisticated and scalable environment for cell survival, having proven to be a potential technique in tissue engineering and organ manufacturing.[22-32] In the present study, we have successfully established a 3D liver tumor model through HepG2 cell loaded sodium alginate/gelatin/fibrin hydrogel printing. Matrix material is an indispensable component in constructing the *in vitro* 3D liver tumor model, taking the effect of supplying the cells with a proper growth and communication environment. The combined sodium alginate/gelatin/fibrin hydrogel has been proven to be an excellent matrix material considering their formability and cytocompatibility with the SEM and AO/PI images.

The biological characterization results indicated that HepG2 cells in the printed 3D liver tumor model grew very well with super livability (100%). The shapes of the HepG2 cells loaded in the 3D liver tumors model changed from separated spheroids to small clusters, and gradually to large hepatocellular carcinoma tissues after two weeks *in vitro* culture, having significantly difference compared with those in the 2D cultures. Both the AFP assay levels of HepG2 cells in the 3D and 2D cultures increased at first but reduced over time. There was an interesting phenomenon in the AFP expression levels of the 3D and 2D models after 5 days *in vitro* cultures, demonstrating that different cell culture modes (2D and 3D) did lead to different AFP results.

Comparing the results of the HepG2 cells in the 2D and 3D conditions, we could suppose that there existed certain death signal transferring from the dead cells to the adjacent living cells. Each cell in the 2D condition was nearly subjected to the same drug action. However cells in the 3D liver tumor model, either encapsulated in the sodium alginate/gelatin/fibrin matrix material or surrounded by other cells in three dimensions, hampering the drug effect to some extent. The death of the whole cell cluster was gradually arising from the outside to inside relying on the death signals transferring. So cells in the clusters were easily collectively dead once one of them died firstly. Cell states in the 3D liver tumor model were much stabler than those in the 2D condition. These differences demonstrated the unreliability of the drug screening results got in the 2D condition. In contrast, drug screening results in the 3D model was more trustworthy for the cell survival microenvironment created was much closer to those in the human body, and the drug action mechanisms were much closer to their native counterparts.

CONCLUSIONS

Common anti-cancer drugs, such as MMC, 5-FU, and MMC+5-FU, were utilized to test the sensitivity of the printed HepG2 cells. HepG2 cells cultured in 2D condition underwent the same anti-cancer drugs were used as a control. In general, the HepG2 cells cultured in different culture conditions performed different drug sensitivities for MMC, 5-FU or their combination. The resistance of the HepG2 cells cultured in the 3D liver tumor model to MMC was weaker, but its resistance to 5-FU was stronger comparing with that in the 2D condition. These results were further verified by the IC50 values with the anti-cancer drugs. Through the analysis of the AO/PI staining results, we concluded that dead cells were attributed to the anti-cancer drugs and the death signals transferred to the adjacent living cells from the dead cells. When the anti-cancer drugs act directly on the surface cells of the 3D liver tumor and 2D monolayer models, the internal cells encapsulated in the sodium alginate/gelatin/fibrin in the 3D liver tumor model could be hampered from the drug effects, and the cell states were much stabler than those of the 2D condition. Compared to the control 2D model, the 3D liver tumor model designed in this article is a relative ideal model for drug screening.

ACKNOWLEDGMENT

The work was supported by grants from the Cross-Strait Tsinghua Cooperation Basic Research (No. 2012THZ02-3), Beijing Municipal Natural Science Foundation (No.

3152015), National Natural Science Foundation of China (NSFC) (No. 81571832 & 81271665 & 30970748), International Cooperation and Exchanges NSFC and Japanese Society for the Promotion of Science (JSPS) (No. 81411140040), State Key Laboratory of Materials Processing and Die & Mold Technology, Huazhong University of Science and Technology (No. 2012-P03), and the National High Tech 863 Grant (No. 2009AA043801).

COMPETING INTERESTS STATEMENT

The authors declare that they have no competing financial interest.

[#] **Both authors contributed equally to this study.**

REFERENCES

1. Munos B. Lessons from 60 years of pharmaceutical innovation. Nature reviews Drug discovery., 2009; 8(12): 959-968.
2. Hutmacher DW, Loessner D, Rizzi S, et al. Can tissue engineering concepts advance tumor biology research? Trends Biotechnol., 2010; 28: 125-133.
3. Elliott NT, Yuan F. A review of three-dimensional *in vitro* tissue models for drug discovery and transport studies. Journal of Pharmaceutical Sciences, 2011; 100(1): 59-74.
4. Mulhall HJ, Hughes MP, Kazmi B, et al. Epithelial cancer cells exhibit different electrical properties when cultured in 2D and 3D environments. Biochim Biophys Acta., 2013; 1830(11): 5136-5141.
5. Hutmacher DW. Biomaterials offer cancer research the third dimension. Nat Mater., 2010; 9: 90-93.
6. Goodman TT, Ng CP, Pun SH. 3-D tissue culture systems for the evaluation and optimization of nanoparticle-based drug carriers. Bioconjug Chem., 2008; 19: 1951-1959.
7. Lee J, Cuddihy MJ, Kotov NA. Three-dimensional cell culture matrices: state of the art. Tissue Engineering Part B: Reviews., 2008; 14(1): 61-86.
8. Griffith LG, Swartz MA. Capturing complex 3D tissue physiology in vitro. Nature reviews Molecular cell biology, 2006; 7(3): 211-224.
9. Yamada KM, Cukierman E. Modeling tissue morphogenesis and cancer in 3D. Cell., 2007; 130(4): 601-610.
10. Damania A, Jain E, Kumar A. Advancements in in vitro hepatic models: application for drug screening and therapeutics. Hepatology International., 2014; 8(1): 23-38.
11. Pampaloni F, Reynaud EG, Stelzer EHK. The third dimension bridges the gap between cell culture and live tissue. Nature reviews Molecular cell biology., 2007; 8(10): 839-845.

12. Zhao X, Du S, Chai L, et al. Anti-cancer drug screening based on a adipose-derived stem cell/hepatocyte 3D bioprinting technique. Journal of Stem Cell Research & Therapy., 2015; 5(4): 273. doi:10.4172/2157-7633.1000273.
13. Yan Y, Wang X, Pan Y, et al. Fabrication of viable tissue-engineered constructs with 3D cell-assembly technique. Biomaterials, 2005; 26(29): 5864-5871.
14. Yan Y, Wang X, Xiong Z, et al. Direct construction of a three-dimensional structure with cells and hydrogel. Journal of bioactive and compatible polymers., 2005; 20(3): 259-269.
15. Wang X, Yan Y, Pan Y, et al. Generation of three-dimensional hepatocyte/gelatin structures with rapid prototyping system. Tissue engineering., 2006; 12(1): 83-90.
16. Li S, Xiong Z, Wang X, et al. Direct fabrication of a hybrid cell/hydrogel construct by a double-nozzle assembling technology. Journal of Bioactive and Compatible Polymers., 2009; 24(3): 249-265.
17. Hull C, Feygin M, Baron Y, et al. Rapid prototyping: current technology and future potential. Rapid Prototyping Journal., 1995; 1(1): 11-19.
18. He K, Wang X. Rapid prototyping of tubular polyurethane and cell/hydrogel constructs. Journal of Bioactive and Compatible Polymers., 2011; 26(4): 363-374.
19. Huang Y, He K, Wang X. Rapid prototyping of a hybrid hierarchical polyurethane-cell/hydrogel construct for regenerative medicine. Materials Science and Engineering: C 2013; 33(6): 3220-3229.
20. Wang X, Paloheimo KS, Xu H, et al. Cryopreservation of cell/hydrogel constructs based on a new cell-assembling technique. Journal of Bioactive and Compatible Polymers., 2010; 25(6): 634-653.
21. Gaetani R, Doevendans PA, Metz CHG, et al. Cardiac tissue engineering using tissue bioprinting technology and human cardiac progenitor cells. Biomaterials., 2012; 33(6): 1782-1790.
22. Wang XH, Tuomi J, Mäkitie AA, et al. The integrations of biomaterials and rapid prototyping techniques for intelligent manufacturing of complex organs. In: Lazinica R, ed. Advances in Biomaterials Science and Applications in Biomedicine. INTECH (www.intechopen.com), 2013; 437-463.
23. Wang XH. Intelligent freeform manufacturing of complex organs. Artificial Organs., 2012; 36: 951-961.
24. Wang XH, Zhang QQ, Overview on "Chinese-Finnish workshop on biomanufacturing and evaluation techniques". Artificial Organs., 2011; 35: E191- E193.
25. Wang XH, Yan YN, Zhang RJ. Gelatin-based hydrogels for controlled cell assembly. In:

Ottenbrite RM, ed. Biomedical Applications of Hydrogels Handbook. New York: Springer, 2010; 269-284.

26. Liu L, Wang XH. Organ manufacturing. In: Organ Manufacturing (XH Wang ed), Nova Science Publishers Inc, NY, USA, 2015; 1-28.
27. Wang XH. Editorial: Drug delivery design for regenerative medicine. Current Pharmaceutical Design., 2015; 21(12): 1503-1505.
28. Libiao Liu, Wang XH. Creation of a vascular system for complex organ manufacturing. International Journal of Bioprinting., 2015; 1(1): 77-86.
29. Xu YF, Wang XH. Application of 3D biomimetic models for drug delivery and regenerative medicine. Curr Pharm Des., 2015; 21(12): 1618-1626.
30. Liu LB, Zhou XW, Xu YF, et al. Controlled release of growth factors for regenerative medicine. Curr Pharm Des., 2015; 21(12): 1627-1632.
31. Wang XH, Yan YN, Zhang RJ. Recent trends and challenges in complex organ manufacturing. Tissue Eng Part B., 2010; 16: 189-197.
32. Wang XH, Yan YN, Zhang RJ. Rapid prototyping as tool for manufacturing bioartificial livers. Trends in Biotechnology 2007; 25(11): 505-513.
33. Wang X, Huang Y, Liu C. A combined rotational mold for manufacturing a functional liver system. Journal of Bioactive and Compatible Polymers., 2015; 39(4): 436-451.
34. Zhao X, Liu L, Wang J, et al. In vitro vascularization of a combined system based on a 3D bioprinting technique. Journal of tissue engineering and regenerative medicine 2014; DOI: 10.1002/term.1863.
35. Wang XH. Spatial effects of stem cell engagement in 3D printing constructs. J Stem Cells Res Rev & Rep., 2014; 1(2): 5-9.
36. Zhao XR, Wang XH. Preparation of an adipose-derived stem cell/fibrin- poly(DL-lactic-co-glycolic acid) construct based on a rapid prototyping technique. Journal of bioactive and compatible polymers., 2013; 28(3): 191-203.
37. Wang XH, He K, Zhang WM. Optimizing the fabrication processes for manufacturing a hybrid hierarchical polyurethane-cell/hydrogel construct. Journal of bioactive and compatible polymers., 2013; 28(4): 303-319.
38. Wang XH. Overview on biocompatibilities of implantable biomaterials. In: Lazinica R, ed. Advances in Biomaterials Science and Applications in Biomedicine. INTECH (www.intechopen.com), 2013; 111-155.
39. Xu W, Wang XH, Yan YN, et al. Rapid prototyping of three-dimensional cell/gelatin/fibrinogen constructs for medical regeneration. Journal of bioactive and

compatible polymers., 2007; 22(4): 363-377.

40. Zhao LH, Li Q, Lin P, et al. Cytotoxicity of astragalus polysaccharides combined with cisplatin of human BEL-7404 hematoma combined with cisplatin on tumor cells. The Practical Journal of Cancer., 2005; 20: 34-35.
41. Stefaniuk P, Cianciara J, Wiercinska-Drapalo A. Present and future possibilities for early diagnosis of hepatocellular carcinoma. World journal of gastroenterology: WJG., 2010; 16(4): 418.
42. Gupta S, Bent S, Kohlwes J. Test characteristics of α-fetoprotein for detecting hepatocellular carcinoma in patients with hepatitis C: a systematic review and critical analysis. Annals of Internal Medicine., 2003; 139(1): 46-50.
43. Bosch FX, Ribes J, Díaz M, et al. Primary liver cancer: worldwide incidence and trends. Gastroenterology., 2004; 127(5): S5-S16.